

Emerging Trends in Terahertz Metamaterial Applications

Balamati Choudhury¹, Sanjana Bisoyi¹, Pavani Vijay Reddy¹, Manjula S.¹
and R. M. Jha¹

Abstract: The terahertz spectrum of electromagnetic waves is finding its position in various applications of day to day life because of its unique properties, including the penetration through opaque materials. Naturally occurring materials in this range are rare due to the display of a natural breakpoint of both electric, and magnetic resonances in these materials. However recent advances in artificially engineered materials, which show resonance in this region are able to harness desirable properties in the terahertz region. In this paper, terahertz design and fabrication issues have been explored along with their applications. A brief review of metamaterial terahertz applications has been carried out including metamaterial absorbers, filters, modulators, switches, lenses, and cloaking structures. The various patterns of metamaterial unit cells are discussed elaborately along with the possibility of flexible active terahertz structures.

Keywords: Terahertz, TDS, metamaterial, absorbers, lenses.

1 Introduction

Terahertz electromagnetic spectrum refers to the range of frequencies that lies within the microwave and infra-red bands, *i.e.* 0.1-10 THz (Figure 1). While systems and applications operating in the micro-wave and IR ranges have been well established over decades, the development of terahertz technology has been slow. Despite its slow growth in the past, research and development of terahertz technology is now growing rapidly. By extending the potential applications of terahertz to biomedical imaging, security etc., this technology is now influencing everyday lives. Design of high performance devices operating in this range of spectrum is achieved only when highly resonant structures are used; this poses a challenge as such naturally occurring materials are rare. Therefore, the techniques to combat this challenge using artificially engineered materials called metamaterials are explored in this paper.

¹ Centre for Electromagnetics, CSIR-NAL, India.

An extensive literature survey has been carried out and reported along with the challenges in various aspects of design bulk fabrication measurement etc. The applications such as terahertz absorbers, amplifiers, filters, lenses switches etc. are discussed elaborately along with the possibility of flexible active terahertz structures. Some novel possibilities such as cloaking and meta-foil are also mentioned in the paper.

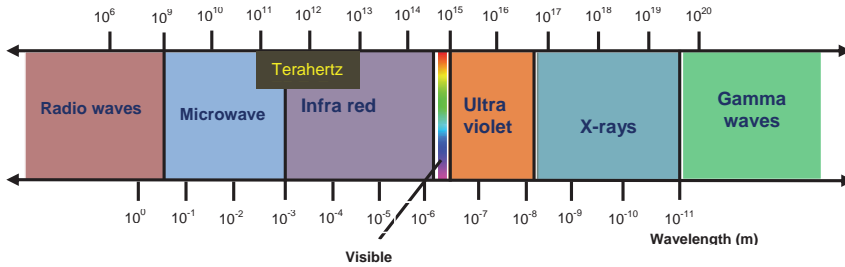


Figure 1: The electromagnetic frequency spectrum.

2 Challenges in terahertz technology

It is seen that the absorption coefficient of terahertz radiation in water ranges between 100 and 1000 cm^{-1} [Siegel *et al.* (2004)]. Therefore, terahertz radiation suffers from very high attenuation during propagation in the atmosphere. In an article titled “*The Truth about Terahertz*” published in IEEE Spectrum in August 2012, Carter Armstrong examines the possible applications, areas of future work and limitations of terahertz technology. He observed that a 1THz signal transmitted at 1W retains only 10^{-13} percent of its signal at a distance of 1km. This implies the need for very high transmission power. Hence, terahertz radiation is not used for long distance communication or radar applications.

Recent advances in the field of terahertz sources and novel terahertz materials have brought about potential applications in earth based systems that take advantage of the otherwise cons of terahertz [Smith *et al.* (2004); Ferguson and Zhang (2009)]. These applications are primarily based on molecular sensing and can be used in environmental, biotechnological, security and bio-medical applications [Maagt (2007)]. Further, imaging in the terahertz offers a higher resolution compared to microwave frequencies as the diffraction limit is given by 1.22λ . However, while IR, optical, and MRI systems are known to provide resolution greater than terahertz, the latter offer better contrast and hence is more useful for distinguishing substances [Siegel *et al.* (2004)].

2.1 Natural breakpoint

Apart from a dearth of naturally occurring sources, one of the biggest factors that limited progress in the area of terahertz technology was the lack of naturally occurring material that exhibit either a strong dielectric response or a magnetic response [Smith *et al.* (2004)]. This feature is seen in the 1-3THz band of the spectrum thereby earning it the name “terahertz gap” – a region where both electric resonance (a characteristic of high frequency) and magnetic resonances (a characteristic of low frequency) die out (Figure 2). This challenge has been overcome by the development of metamaterials – artificially engineered materials that can be design to exhibit strong electric and magnetic resonances.

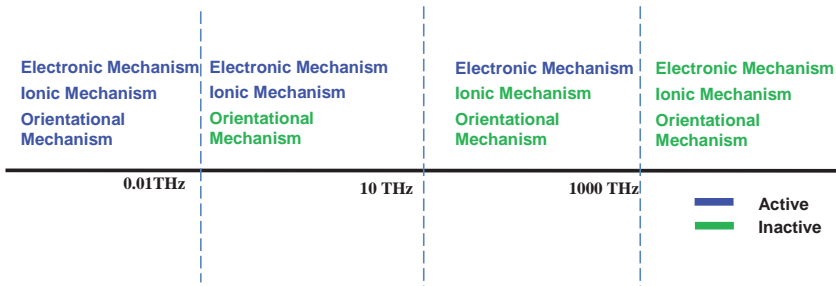


Figure 2: Atomic polarization of dielectrics at higher frequencies.

2.2 Design issues

The EM design of metamaterial subwavelength structures follows techniques similar to those used in microwave design. Further, the EM designs can be scaled down to achieve terahertz metamaterial structures [Capolino (2009)]. Most of the EM designs reported in literature used the scaling down technique whose validity was proved through experimental results. Hence, methods like ECA analysis, FDTD methods, and LC-MTM techniques can be used for analysis of metamaterial structures at terahertz frequency.

2.3 Fabrication issues

Terahertz metamaterials are subwavelength structures, the feature size of which is often in the micrometer range. Fabrication of these structures with minimum expense while maintain high levels of precision is a challenge that has to be overcome in order to avail extensive usage of this technology in commercial applications. It has been reported that even small discrepancies in feature size can produce results

that are in disagreement with simulated results [Hokmabadi *et al.* (2013b)]. Further, traditional fabrication procedures involving photolithography hamper mass production of metamaterials [Xie *et al.* (2009)]. However, improvements in nanotechnology are now enabling the production of devices that can work up to even the far end of the terahertz spectrum and in the IR and even possibly the optical regime [Hess *et al.* (2012)]. A few articles that describe challenges of fabrication are mentioned in this section.

Chicki *et al.* (2009) demonstrated the use of electron beam lithography (EBL) for the fabrication of terahertz metamaterial structures. The process was discussed in detail and it was seen that large, defect-free structures can be developed using this technique. Prior to the fabrication, the structure, a split ring resonator resonating at 1THz, was simulated on CST Microwave Studio and the effect of substrate doping on the resonant frequency was studied. The resonant frequency was seen to shift to the left with increase in the substrate conductivity.

Singh *et al.* (2010) measured and demonstrated optical properties of planar thin-film metamaterials using terahertz time-domain spectroscopy at room and liquid nitrogen temperatures. Photolithographic technique was used to fabricate the metamaterial – a 150 nm thick layer of aluminium was deposited in a silicon substrate of thickness 640 μm . The system resonated at 0.5 THz and there was an increase in Q-factor because of decrease in temperature. It was seen that thicker metal films increase the Q factor by 40%, thereby reducing the losses. Further, the same group has demonstrated the technique of fiber drawing as a method for producing double split ring magnetic metamaterial in terahertz range; a technique commonly used for producing split ring resonators [Singh *et al.* (2012)]. Transmittance obtained from numerical simulation was found to match with experimental results. Further, it is proposed that this technique can be applied to more complex structures.

Shin *et al.* (2010) investigated various MEMS techniques for fabrication of electronic circuits built in a 0.22 THz travelling wave tube (TWT) amplifier. Four different techniques were investigated towards fabrication of metamaterial based electronic circuits' viz. KMPR UV LIGA, SU8 UV LIGA, high precision CNC nano-machining, and silicon-molded electro-deposition.

Tao *et al.* (2010) reported the fabrication and EM characterization of metamaterial structure for a large area. The designed structures were placed on biocompatible silk substrates. Electromagnetic response of the metamaterial silk composites was characterized and manipulated using terahertz time-domain spectroscopy (THz-TDS). CST Software simulation results showed that for a unit cell having a dimension of 50 $\mu\text{m} \times 50\mu\text{m}$, the resonance occurs at 0.85 THz, which was higher than the resonance frequency of 0.7 THz of a unit cell having a dimension of 100 $\mu\text{m} \times 100\mu\text{m}$. Silk composite metamaterials can be useful in biotracking,

bio-mimicry, silk electronics, and implantable biosensor and bio-detectors.

2.4 Measurement characterization issues

Historically, growth in terahertz technology has been hampered by a lack of sources and detectors; naturally occurring sources are rare in this regime. However, in the past decade or so, development of gyrotrons, backward wave diodes, and resonant tunneling diodes has enabled generation of 0.3-1 THz. Further, mechanisms involving photoconduction and optical rectification have enabled generation of broadband pulsed lasers [Ferguson and Zhang (2009)]. However, the output powers of these sources are generally in the order of μW -mW. Advances in semiconductor technology have led to the design of semiconductor lasers and quantum cascade lasers. However, these technologies require cryogenic cooling.

With sources being capable of generating very low power, detection of THz radiation is an extremely challenging task, requiring detectors with high sensitivity and low loss. Further, background thermal radiation often decreases the quality of the received terahertz radiation. Currently, bolometers that absorb THz radiation are commonly used.

Recent advances have also brought about detectors like single electron detector, heterodyne sensors, coherent detectors (used in THz-TDS systems), thin crystal sensors, photoconductive antennas etc. It has been observed that the EM characterization of most of the metamaterial structures is done using THz-TDS measurement technique. A schematic of the measurement set up is given in Figure 3.

Minowa *et al.* (2008) proposed EM characterization of metamaterial slab using THz time domain spectroscopy. The mathematical formulation for evaluation of effective permittivity and permeability was derived. The experimental results for four different configurations of phosphor bronze wire grid structure operating in THz frequency (0.5 THz to 2.5 THz) range were shown. It was observed that in both the parallel and perpendicular configurations, the magnetic permeability is less than one.

Merbold *et al.* (2011) devised an experiment that enables the spatiotemporal visualization of radiation in metamaterial arrays. This technique also enables the investigation of near-field to far field transition in the case of SRR arrays. In the paper, the experiment was used to study the interaction of radiation as well as verify Babinet's principle in arrays of SRR's and their complementary structure.

Kumara *et al.* (2011) studied the terahertz time dependent magnetic near-field of single split-ring resonators and double split-ring resonators by using Terahertz Time-Domain Spectroscopy (THz-TDS). To determine THz magnetic near-field of metamaterial elements with subwavelength resolution they used a technique, which

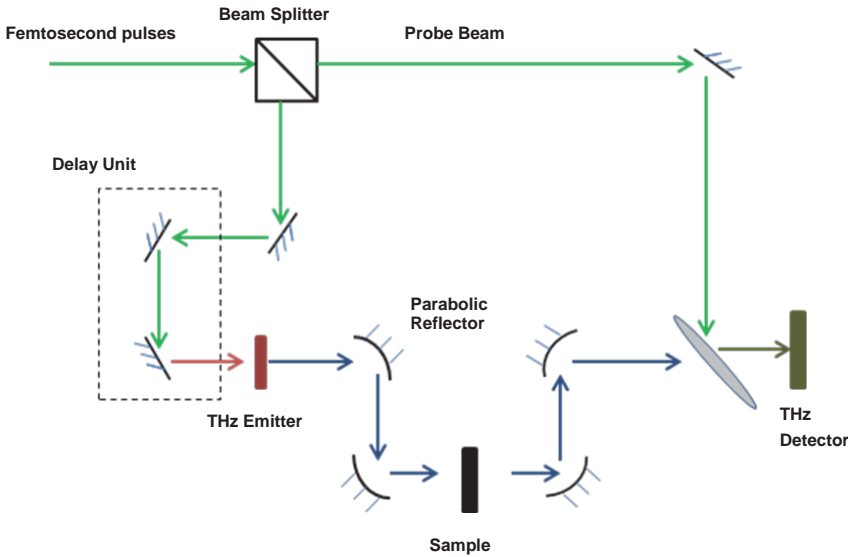


Figure 3: Schematic of terahertz time domain spectroscopy (THz-TDS) set up.

will give information about strength and distribution of the local magnetic field.

Measurement of refractive indices of thick and thin film dielectric samples for metamaterial sensor design was demonstrated by Reinhard *et al.* (2012). The sensor was fabricated onto the dielectric using UV-lithography and was designed to operate in the frequency range of 1 THz to 1.6 THz. It was characterized experimentally by conducting reflection measurements with a THz time domain spectroscopy. A thickness resolution of 12.5nm of the operating THz wavelength and a refractive index resolution of 0.01 for weakly absorbing sample materials was obtained.

3 Terahertz metamaterial design applications

The growing field of terahertz applications includes absorbers, switches, metafoils and terahertz devices such as amplifiers, modulator, lenses, filters etc. The current scenario of these applications is described in this section. Further, an important block of this section also includes the design of terahertz metamaterial structure, which is the building block of the above mentioned applications.

3.1 Metamaterial absorber

An ideal electromagnetic absorber absorbs all the incident electromagnetic radiation, without any transmission or reflection. Material properties such as effective permittivity and permeability, thickness, and morphology of the EM design are the most important parameters that affect the performance of an absorber. This section explores the trends in terahertz metamaterial absorber design and applications to various fields.

3.1.1 Biomedical applications

The terahertz range of frequencies is slowly finding applications in day to day lives. One such application with great potential is imagining using terahertz for biomedical applications. Terahertz can be used to obtain high contrast images that can be used for characterization of tissue and detection of skin diseases.

Choudhury *et al.*, (2013b) proposed a novel metamaterial RAM (absorber) design with efficiency as high as 99.32% over the bandwidth required for biomedical terahertz application. The performance is enhanced by a significant amount by introducing an optimized metamaterial SRR layer (Figure 4). The particle swarm optimization (PSO) algorithm was used to retrieve the structural parameters at the desired resonant frequency. At 1.16 THz the absorption was 99.32 %, which is sufficient for biomedical spectroscopy applications (Figure 5).

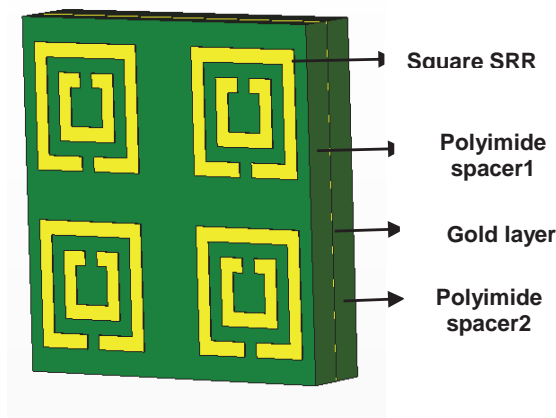


Figure 4: The four layer Metamaterial RAM design. The top layer consists of four optimized square SRR structures.

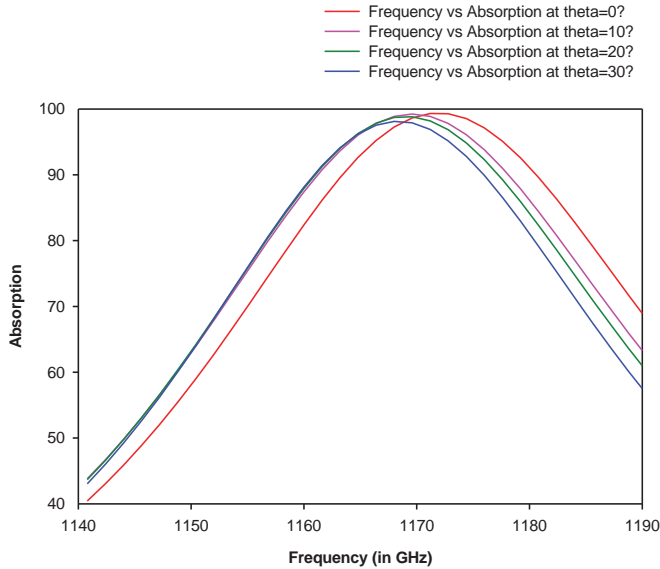


Figure 5: Absorption characteristics of the RAM (absorber) designed by soft computing PSO algorithm.

3.1.2 Space applications

Historically, terahertz technology has been employed in space based applications like earth observation science, radio astronomy and planetary/cometary science. In fact, terahertz spectroscopy offers an insight into the physical condition (heat, pressure etc.) as well as molecular concentration of the region being observed. This property is attributed to the fact that terahertz photons are emitted during changes in a molecular, rotational or bending state of atoms [Maagt (2007)]. Terahertz systems have already been deployed in missions like the NASA Cosmic Background Explorer (COBE), Microwave Instrument for the Rosetta Orbiter (MIRO) etc.

Shchegolkov *et al.* (2009) designed and manufactured a set of four perfect sub-wavelength film absorbers. Absorbers were composed of a simple metallic FSS on a lossy dielectric film and a metal ground plane. Standard microfabrication technique was used for fabrication of a fishnet like absorber. FEM based simulation results showed that absorption was close to 100% for very large angles of incidence at a frequency 0.73 THz. Fishnet absorbers are easy to manufacture and can be utilized in emissivity spectrum modifiers, bolometer-type detectors, non-reflecting surfaces, thermal imaging, and narrow-band THz sources. Low self-heat capacity makes these absorbers, combined with thermo detectors, especially attractive for

precise frequency-selective detection of THz radiation.

3.1.3 Security applications

Apart from biomedical spectroscopy, terahertz imaging in space science, stealth technology, electromagnetic shielding of high reflection surfaces is an important application where EM absorbers are used. Further, terahertz radiation can be used for distinction of unauthorized materials such as weapons, knives, drugs and explosives in airports where near field imaging is of great interest [Hashimsony *et al.* (2001)].

Tao *et al.* (2008b) proposed a flexible thin metamaterial absorber, which operates at very wide angle of incidence (Figure 6a). The designed metamaterial absorber results in 97% absorption at 1.6 THz (Figure 6b). Further, the fabrication and measurement results were presented, which has an excellent agreement with the simulation results.

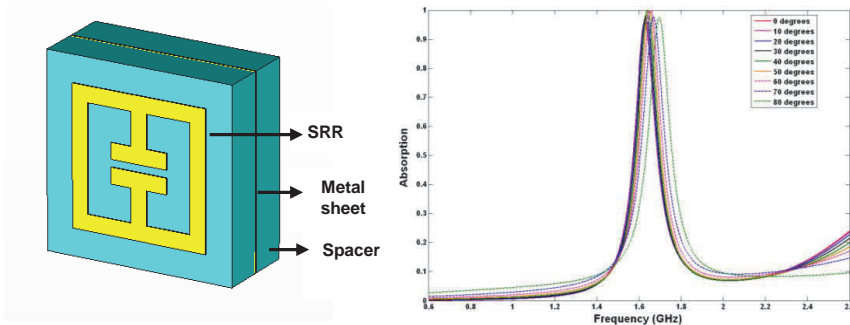


Figure 6: (a) Design of the terahertz metamaterial absorber (b) Absorption characteristics of the absorber.

Gu *et al.* (2010) designed a wideband metamaterial absorber that resonates at 4.28 and 4.68 THz. The absorption characteristic shows more than 90% absorption at 0.70 THz and the maximum absorption are mainly due to metallic absorption. This type of absorber can be used in various applications like thermal detector and THz stealth technology.

Noor *et al.* (2010) reported a wideband, wide angle terahertz absorber using a Hilbert curve array of metamaterial structures. Normal THz absorbers are relatively narrow band. Simulations were done using Ansoft's HFSS by considering a single unit cell. For normal incidence, wide absorption bandwidth was more than 100%. Compared to other terahertz absorbers, this absorber showed much wider

bandwidth having more than 90% absorption at 60 and 45 degrees. The simulation results showed that peak absorption was very high, *i.e.* 98% for normal incidence and varies between 86% and 94% for oblique incidence.

He *et al.* (2011) introduced a dual-band metamaterial absorber with polarization insensitivity and wide incident at terahertz frequency range. Absorption characteristics of the absorber were evaluated for differently polarized and incident directions of incident TE and TM wave. Hence from the experiment and calculation results they found two absorption peaks of 82.8% and 86.8% at 1.724 THz and 3.557 THz respectively, for fabricated absorber.

Park *et al.* (2011) presented a power-meter using metamaterial-inspired thin-film absorbers operating from 0.1 to 0.2 THz. The terahertz power-meter was fabricated using a conventional micro-fabrication method and has two parts - a bolometer and a cavity. The absorbing layer consists of a low loss, thin dielectric membrane onto which thin metallic layers are patterned. At 220 GHz absorption coefficient is above 0.75.

Huang *et al.* (2012) presented the optimization of flat broadband terahertz absorber by the application of a hybrid algorithm, which integrates Differential Evolution Strategy (DES) and Continuous Ant Colony Optimization (CACO). The optimized absorber consists of three I-shaped resonators and it is seen that the absorption is above 90% for a bandwidth ranging between 0.872 THz and 0.975 THz.

Zhang *et al.* (2012) designed an electromagnetic wave absorber with broad bandwidth at terahertz frequency using circular metallic patches. Micro-fabrication method was used to fabricate the structure as it is simple and has fair fabrication robustness. Simulations were done for the designed structure using terahertz time domain spectroscopy (THz-TDS) with magnetic field distribution at three different frequencies, *i.e.*, at 0.54 THz, 0.64 THz and 0.67 THz.

Yang *et al.* (2013) proposed a tunable metamaterial absorber in the frequency range of 1.08 THz to 1.20 THz. The tuning was achieved through MEMS actuators. The absorption throughout the frequency range was 98% and at 1.297 the peak absorption was 99.9%. The fabrication procedure for the same was also discussed.

He *et al.* (2013) proposed a novel broadband absorber design using a pyramidal graphene-dielectric multilayer backed by a thin metallic film. The pyramidal graphene-dielectric multilayer provides an anisotropic permittivity. Absorption of around 93% is achieved over a broadband with a dip of absorption in between. To remove the dip, a rectangular stack was added to the frustum of pyramidal stack. The simulation results from 8 THz to 100 THz are reported. It was observed that with a changed dimension of pyramidal graphene-dielectric multilayer, absorption in lower frequencies also can be obtained.

Hokmabadi *et al.* (2013a) used frequency selective surfaces for design of absorbers followed by a review on metamaterial terahertz absorbers [Hokmabadi *et al.* (2013b)]. The analysis of RLC model of the absorber was carried out and a curve fitting solution is provided to achieve optimum absorption, *i.e.* 97.5%. For various thickness of the spacer, it has been observed that the resonance frequency changes.

Hu and Li (2013) designed and fabricated a terahertz absorber using square split ring resonators. The resonant characteristic of the split ring resonators was calculated using equivalent circuit analysis method. Simulation of the absorber was carried out using three types of dielectric spacers, *viz.* GaAs, polyimide and silicon. High-resistivity and high-purity silicon was found to be excellent for terahertz transmission due to its nondispersive nature and low absorption in terahertz region. The simulation results show maximum absorption of 99.3% at 0.575 THz, and a full width at half maximum bandwidth of 50 GHz.

Kearney *et al.* (2013) designed a terahertz absorber with a Ti conductive layer. The thickness of the resistive spacer was optimized to achieve optimum absorption. The results of finite element simulations and the measured results reveals that a very thin Ti layer of 1270 nm deep into the SiO₂ layer gives 94% of absorption.

Kung and Kim (2013) proposed the design and analysis of a broadband absorber for biomedical imaging and sensing applications. A thin, tuneable metamaterial absorber was designed and the bandwidth was doubled by optimizing the outer ring of the FSS structure. A method for tuning was explained through multilayer FSS ring structures where the resonant frequency changes with change in radii of the front ring.

Mo *et al.* (2013) proposed a broadband absorber using a thin silicon dioxide film as spacer. Different sizes of aluminium cubes were placed above the dielectric spacer to achieve a bandwidth of 200 GHz. The various peaks of absorption of 99.83% and 98.67% were observed at 2.58 THz and 2.65 THz respectively.

Yang *et al.* (2013) designed and discussed the fabrication of a tunable metamaterial absorber employing MEMS based actuation. The basic structure of the metamaterial is formed by two back to back split ring resonators separated from a ground plane by a dielectric. One of the split rings is placed on a movable beam. Hence the resonant frequency of the metamaterial is varied by changing the distance between the two rings. Different MEMS based actuation techniques are suggested for controlling the beam. On simulation, it was observed that as the distance between the two rings was varied from 0-5 μm , the resonant frequency changed from 1.08 THz to 1.20 THz.

Wang *et al.* (2014) designed a tuneable terahertz absorber by varying the effective

length of the absorber. The effective length was varied by mechanically shifting a movable surface along with a fixed section of the absorber. Through this mechanism they achieved at about 23% tunability in the frequency band of 2.11 to 2.59 THz.

3.2 Terahertz Devices

As systems are being developed for terahertz applications, it is necessary to develop devices that can control and condition the generated or received radiation. Typically, this requires devices like switches, modulators etc. This section reviews the trends of terahertz devices those includes modulators, amplifiers, filters, lenses etc.

3.2.1 Modulators

The terahertz modulators play a vital role in a THz-TDS measurement system. Further, towards broadband applications it is required to have tunable terahertz modulators. Electrically controlled solid state phase modulators were demonstrated using hybrid metamaterial structures [Chen *et al.* (2009a)]. The electrical tuning of the modulator makes it suitable a candidate for broadband applications and can replace mechanical choppers. THz TDS was used for measurement and EM characterization of the structure.

Padilla *et al.* (2009) designed an active terahertz metamaterial device that offers real time tuning using Schottky diodes to manipulate the substrate properties. The structure demonstrated 50% modulation in the transmitted intensity and hence can be used in the design of filters. Further, the potential of the structure for operation as a modulator was discussed. The compatibility of the fabrication of the structure with contemporary semi-conductor fabrication techniques was also presented.

Paul *et al.* (2009) designed a polarization independent terahertz modulator. The structure consisted of an array of gold cross on an n-doped GaAs substrate, which is externally biased. The crosses are interconnected using $1\mu\text{m}$ wires. For THz frequencies, the structure was seen to be transparent during forward bias and negative during negative bias. Therefore, structure can modulate THz waves if the bias is a modulating signal. The modulation speed was studied for modulating signals up to 100 kHz. A cutoff frequency of 80 kHz was observed, which is much greater than that of semi-conductor based modulators. Further, symmetric structure renders the metamaterial polarization independent.

A feasibility study of a zero-index terahertz Quantum-cascade laser, based on a CRLH resonator was carried out by Tavallae *et al.* (2010), which exhibits a uniform spatial mode that is immune to spatial hole burning. Full wave simulation

of the metamaterial was done by commercial finite element electromagnetic solver. The simulation results showed that the system supported backward waves below 1.9 THz while above 2.23 THz forward waves are supported. For zeroth-order resonance threshold gain value was increased by a factor of 1.5 to 2 when CRLH-based QC resonator was used.

Minowa *et al.* (2011) examined the waveguiding properties of a planar metamaterial slab using terahertz time-domain attenuated total reflection spectroscopy. Splitting resonator (SRR) structure is presented to calculate strong Lorentz-type resonances at the desired frequencies. Resonant excitation of waveguide modes in the slab were shown for transverse electric and transverse magnetic excitation of evanescent waves.

Shin *et al.* (2011) presented a novel RF waveguide composed of photonic crystal (PC) metamaterial slabs used for terahertz (THz) sheet beam device applications. They examined metamaterial RF structures, the study of which was extended to NIMs, consisting of SRR and wire arrays, which was embedded into the PC waveguide.

Sheng *et al.* (2011a) presented a terahertz wave modulator based on a microstrip resonator structure, which can achieve terahertz wave signal modulation. This is based on the resonance characteristic of the microstrip structure which is handled by modulated laser. Hence, after examination, the modulation speed and attenuation was found to be 0.1Kb/s and 25dB respectively at a frequency of 0.32 THz.

Koutsoupidou *et al.* (2012) presented a THz imaging system for bio-medical applications using planar antennas with metamaterial substrates as emitters. The imaging system consists of a THz source, detector and an arrangement of lenses. A rectangular patch antenna and bow-tie patch antenna printed on metallic split ring resonators are used as THz sources. Photolithography or electron beam lithographic processes are used for the fabrication of antenna. The simulations are done for an operating frequency of 1 THz and the designed antennas are analyzed for their performance by comparing its characteristics with a reference antenna. It is observed that the proposed antenna design has more directivity than the reference antenna. The proposed design helps in better imaging of bio-samples. Further, gain can be improved by using spiral or log- periodic patch antennas.

Rout *et al.* (2010) proposed an advanced technique of achieving active terahertz modulation through embedded high electron mobility transistor (HEMT). A double electric split ring resonator was designed using a gold layer and a GaAs HEMT was used beneath the split gap of the resonator. The property of this transistor was changed by changing the gate bias voltage of the HEMT switch. TDS system was used for EM characterization. The designed modulator was demonstrated at 0.55

THz.

Starinshak *et al.* (2007) investigated the effects of metamaterial in terahertz travelling wave tube amplifier. They designed sub wavelength holes in the lattice and tested the TWT amplifier at 0.4 THz. As there was no significant change in the magnitude of axial field alternative shapes of holes were investigated through microfabrication. Simulation results and preliminary studies in corrugated beam tube with slots were shown with a suggestion of further warranty in the implementation because of inconsistency between repeated simulation results.

3.2.2 Bolometer

Bolometers and emitters are the most important devices in a terahertz spectroscopy system. Strikwerda *et al.* (2011) realized metamaterial enhanced THz radiation detector with optical read-out. Split ring resonators were used to find the resonant response that can be optimized for specific design frequencies. Bi-material cantilever pixels were used to fabricate metamaterials for operation at 95 and 693 THz, which can be used for radiation sensing and detection.

Alves *et al.* (2012) designed narrowband terahertz emitters using metamaterial films for a bandwidth of 1 THz. Three different samples, each which radiates at a different frequency between 4 and 8 THz, were designed. The designed emitters were also tested at three different thermal levels, viz. 140°, 280° and 400°C. It was seen that the absorption spectra of the metamaterial agrees well with emitted radiation in accordance with Kirchoff's law. Further, Planck's law could be approximated to the Rayleigh-Jeans limit since the emitted power increases linearly with temperature. A complex design of the metamaterial structure for multiband operation was also demonstrated along with measurement results.

Kan *et al.* (2012) demonstrated Smith-Purcell effect using electron bunch and metallic grating to produce terahertz waves. The use of electron bunches along with a metallic grating of 2mm produced radiation at a frequency less than 0.7 THz. The output was measured using a bolometer at three different radiation angles, *i.e.*, at 54°, 70°, 110° and the maximum output is observed at 54°. Further, new terahertz devices can be developed using similar schemes.

3.2.3 Filters

Filters are the widely used devices in various applications of spectroscopy, imaging and molecular sensing. Lu *et al.* (2010) demonstrated the behavior of a high-order, broadband THz band pass filter which was realized by a complementary, multi-layer metamaterial structure. Ansoft HFSS was used for simulation and a transmission band from 227GHz to 283 GHz was observed with two transmission peaks at around 260GHz. There was a good agreement between theoretical and

experimental results. Simulation results showed that the metamaterial filter had a flatter and wider passband, steeper skirts, and much better out-of-band rejection.

Chen *et al.* (2011) examined the utilization of metamaterial resonators as bandpass filters and showed the control of surface electromagnetic waves (SEW) with novel metamaterial elements. They used a single planar wire transmission line, *i.e.* Planar Goubau Line (PGL) to get wide-band surface-electromagnetic wave spectrum in gigahertz (GHz) and terahertz (THz) frequencies via a coplanar waveguide coupler with 50Ω impedance. Two independent configurations of coupled metamaterial elements that sustained flat transmission spectrum of the PGL were taken, which showed the use of this configuration for high bandwidth terahertz communications. Further the concept was used by Horestani *et al.* (2013) for design of a compact band pass filter using PGLs. The focus of the work was on applications of SRR structures in design of third-order periodic bandpass filters and coupled-resonator bandpass filters. Equivalent circuit analysis of SRR has been done and a third-order periodic bandpass filter based on SRR/gap-loaded PGL was demonstrated through simulation and experimental results.

Sabah *et al.* (2011a) realized a multilayer metamaterial structure which consists of five layers with chiral and dielectric materials and acts as a terahertz polarization rotator. The spectral-filter and polarization-rotation properties were optimized by combination of chiral and dielectric material. At 0.72 THz bandwidth the structure with chiral material acts as a band pass filter.

Chen *et al.* (2012) analyzed the resonant properties of high-Q membrane metamaterial resonators by way of terahertz time-domain spectroscopy. The resonance strength and the Q-factor of sharp resonance were greatly influenced by the geometry of the resonators, the membrane thickness and dielectric loss. Further, the influence of membrane thickness on the sensitivity was explored and it was found that the high-Q membrane metamaterial sensors with moderate thickness could be a good compromise for ultrathin devices. Integrated terahertz filters and sensors can be developed using such devices.

Basiry *et al.* (2012), proposed the design and optimization of terahertz filters using periodic method of moment. The optimized design was validated using Ansoft HFSS 12. It has been reported that the computation time of PMOM code in conjunction with random hill climbing (RHC) optimization takes 40 sec.

3.2.4 Lenses

One of the most important applications in terahertz technology is design and development of low spatial resolution THz systems. The design and development of THz lenses with strong focusing characteristics will solve the problem. Neu *et al.*

(2010) discussed the optical properties of a gradient index (GRIN) lens which is based on a three-layer metamaterial structure. The lens was designed for operation between 1.2 and 1.5 THz, which permits focusing of terahertz radiation to a spot of diameter of one wavelength.

Alves *et al.* (2013) designed and fabricated bi-material MEMS sensors. SiO_x and Al were used for fabrication of MEMS sensor. The design uses a metamaterial absorber of near unity absorption at 3.8 THz. The sensor shows a high sensitivity value of 1.2 deg/ μ W and time constant as low as 200 ms. Measurement results are in excellent agreement with the FE simulation results. These MEMS sensors arrays are good candidates for THz imaging.

A metamaterial lens was designed by Headland *et al.* (2013) which deflects terahertz beam. The metamaterial lens was designed using a lattice of with varying radii. As the thickness of the flat dielectric slab is less than a millimetre, the lens is very compact. A particular design of the lens to deflect the beam at 45° was shown.

Zhang *et al.* (2013a) designed and fabricated a metamaterial that can be tuned to change its properties from isotropic to anisotropic. The structure consists of rows of gammadion shaped structures. Alternate rows are released from the substrate and can be moved in the lateral direction with the help of electromechanical actuators. This enables the change of the relative positions of the gammadion structures and hence switching between isotropy and anisotropy is possible. This structure enables polarization dependent control over the transmitted wave as well as control on the transmission intensity and phase.

3.3 Terahertz metamaterial structures

Metamaterials may be classified as single negative metamaterials (SNG) or double negative metamaterials (DNG). These properties can be achieved using a number of structures such as the split ring resonators (SRR), artificial magnetic conductor (AMC), high impedance surfaces, frequency selective surfaces (FSS), etc. Some of the typical metamaterial structures are shown below (Figure 7).

3.3.1 Split ring resonators

Moser *et al.* (2005) designed and fabricated an electromagnetic metamaterial using micro-fabrication technique. The design was based on a rod-split ring resonant structure. The response of this structure was numerically simulated and further verified using far IR transmission spectroscopy. It was shown that the composite structure behaves as a metamaterial in the frequency range of 1-1.27 THz. The authors proposed that this micro-fabrication technique can be extended to fabricate meta-material structures that operate in the near IR range of frequencies.

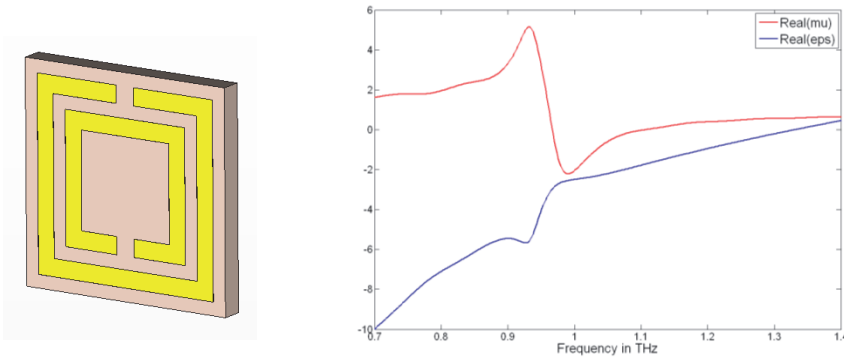


Figure 7: Schematic of typical metamaterial structures (a) Optimized split ring resonator (b) Extracted permittivity and permeability at THz.

Padilla *et al.* (2006) characterized the response of a planar array of split ring resonators embedded in a Gallium Arsenide (GaAs) substrate which works as an absorptive metamaterial at 0.5 THz and 1.6 THz. The dynamic control of the metamaterial by impinging the substrate with light was proposed. The effect of the power of the incident light on the different absorption frequencies was studied.

Hand *et al.* (2008) studied the THz radiation analysis on the fabrication yield of split ring resonator. Hybrid resonators are designed and fabricated to achieve dual band resonance at 1.29 and 1.48 THz. With 100%, 90 % and 60% fabrication yield, the resonance effect is shown. It was observed that the resonance degrades as the manufacturing defects increases. This analysis shows impurity effects because manufacturing defects are more significant at higher frequencies.

Chiam *et al.* (2009) designed a planar metamaterial structure that displayed a transparent window in an otherwise opaque response. This phenomenon of transparency, called electromagnetically induced transparency, is achieved when two parallel polarized waves are incident on the surface and excite resonances in its constituent structures. The structure of the metamaterial consists of a split ring resonator enclosed by a square ring.

Han *et al.* (2009) designed a THz metamaterial structure using close-ring pair with a resonance at normal excitation, unlike previous designs that displayed resonance during in-plane excitation. The structure was simulated as well as fabricated and the value of refractive index was found to be negative at resonant frequency using parameter retrieval methods. Further, a study was conducted to study the effect of geometry on the performance, figure of merit etc.

Sabah *et al.* (2009) studied the evolution of metamaterial design and its applica-

tion in the terahertz regime. They then proposed a wide-band, left handed terahertz metamaterial using two different circular split ring resonators and thin wire elements – designed for resonance at 2.7 THz and 4THz. The combined effect of the two structures resulted in maximum negative refractive index at 3THz and a wider range of frequencies in which the refractive index stayed negative. Further Sabah *et al.* (2011b) presented dual-band polarization-independent fishnet metamaterial for THz frequencies. The structure permits dual-band modes having two resonances in which the first one works in fixed a left-handed mode and the second one works in either as left-handed or single-negative mode. The mode can be selected by changing the substrate properties. The group also discussed multilayer structure formed by metamaterial and dielectric slabs with different material properties [Sabah *et al.* (2011c)]. Chiral and dielectric material together allows optimization of spectral filter and polarization rotation properties of the structure. The structure can be used for filtering, coating, and especially as polarization conversion devices in the THz regime.

Ortner *et al.* (2010) investigated resonant behavior of SRRs and Complementary S-RR (CSRR) by THz time-domain spectroscopy and by THz near-field microscopy. Through measurements, it was verified that the magnetic near fields were responsible for the characteristic response. They developed a THz-near-field imaging method that gives the spatially resolved measurements of the amplitude, phase and polarization of the electric fields and extracted microscopic magnetic near-field signatures. The simulation results showed that numerical simulations agreed with proposed theories and fully agrees with predictions from Babinet's principle.

Wallauer *et al.* (2011) proposed a split-ring resonator based on metamaterial arrays. THz far-field spectroscopy and THz near-field microscopy were used to find out coupling between split-ring resonators. It was seen that for the fundamental LC-resonance the microscopic dipole moments of the individual SRRs form a macroscopic dipole in the collective coupled mode.

Cheng *et al.* (2012) designed and simulated a complementary U-shaped terahertz chiral metamaterial. Due to the chiral configuration, the metamaterial structure possessed negative refractive index. Large circular dichroism, which could vary till -16dB was observed and a strong optical activity at a rotation angle of 53° was seen. The metamaterial structure presented here could be used as a polarizer.

Li *et al.* (2013) designed and fabricated an isotropic dual band terahertz metamaterial using metallic rings. The periodic array of metallic rings result negative permittivity in the frequency bands of 298–388 GHz and 652–780 GHz. The simulation results were well in agreement with the measurement results carried out using time domain spectroscopy.

3.3.2 Hybrid unit cells

Miyamaru *et al.* (2008) proposed an H shaped metamaterial fractal structure for multiband operations. As the resonant characteristics of metamaterial structures depend on the size of the unit cell, three different levels of H patterns were generated and a frequency shift was observed. It was observed that these fractal metamaterial structures could be a good choice for multiband metamaterial devices.

The EM material characterization of a bulk material designed using metallic crosses was carried out by Paul *et al.* (2008). The 3D metamaterial structure of millimeter thickness was fabricated using a multilayer lithography process. The metallic crosses were embedded in benzocyclobutene (BCB)-based resin. The measurement shows negative refractive index in the frequency range of 0.96 THz and 1.17 THz.

Yuan *et al.* (2008) proposed novel terahertz metamaterial thin film designs based on single-particle electric-field-coupled resonators. The first unit cell design was made up of absorbing Kapton layer, which is sandwiched between two layers of gold, one of which has a rectangular opening in it. The second design was cross structure with the same material configuration. Both the designs were fabricated and the second structure was found to be suitable for absorber application. The simulation and measurement result of the metamaterial film based absorber was shown at 1 THz. At normal incidence the absorption was greater than 99%.

Chen *et al.* (2009b) designed a polarization insensitive fish-net type metamaterial structure. On simulation, a higher order resonance was observed along with the expected resonance. This resonance was also believed to be left-handed in nature and the verification of the same was done by studying the currents in the structure and using well-established parameter-retrieval methods.

Cui *et al.* (2010) designed a broadband metamaterial structure with a negative refraction property at multiple bands. The structure operates between 5 to 20 THz and is composed of 3 circular metallic strips with different radii. The structure is insensitive to the displacement of metallic pairs thus providing large fabrication tolerances. The system resonates at least in two frequency bands of 7 and 13 THz.

Lim *et al.* (2010) fabricated a planar hybrid metamaterial with different split ring resonators on silicon substrates by femtosecond (fs) laser micro-lens array (MLA) lithography and lift-off process. Terahertz time domain spectroscopy was used for characterization of electromagnetic field response of these hybrid and single dimension metamaterial structure. Simulation results showed that metamaterial with single SRR design showed single resonance peak at a certain THz frequency. Multiple resonance peaks at different THz frequencies (0.2 to 1.02 THz) were obtained by combination of multiple SRR structures with different dimensions. It is found that interaction among the SRRs in metamaterial creates a strong mutual

coupling within the region between 2 SRRs. To realize a tunable and broad band THz response for the THz detection, sensitivity enhancement approach (Hybrid SRR metamaterial design and fabrication) was provided.

Chowdhury *et al.* (2011) analyzed the coupling between laterally paired terahertz metamaterial split-ring resonators. Tuning of the electric and magnetic coupling parameters can be achieved by design modification at the unit cell level. Depending upon spacing and placement of the SRR gaps, blue shift or red shift of the resonance was observed due to changes in capacitance between the resonators. It is illustrated how coupling may be designed in parallel with polarizability and densities of the unit cells in order to design the macroscopic metamaterial response.

Li *et al.* (2012) designed, simulated, fabricated and tested a dual-band terahertz metamaterial. The metamaterial consists of cruciform and square structures. As a result of this configuration, the negative permittivity was observed in the following bands: 378-500 GHz (due to the cruciform structures) and 626-677 GHz (due to the squares).

Lu *et al.* (2012) proposed the design of a metamaterial with high refractive index at two frequencies. The metamaterial structure has five by five unit cells and is designed using metallic gold structure integrated on a polyimide substrate. Through analysis, a high refractive index was observed at two frequency bands, *i.e.* 61.83 at 0.384 THz, and 19.2 at 1.416 THz respectively. The low refractive index observed at second frequency can be improved by modifying the structure. Further, this method can be extended to design metamaterials of high refractive index with multiple frequencies.

Olifierczuk *et al.* (2012) designed tunable metamaterials using liquid crystals and performed simulations based on In Plane Switching (IPS) mode. The structure consists of a double-split square resonator embedded on a liquid crystal layer. Numerical simulations were done in the frequency range of 0.32THz to 0.44THz to obtain the scattering parameters of liquid crystal for two sizes of split ring resonators. The results show the possibility of tuning the metamaterial parameters around the operating frequency band. This structure has potential applications in filter design, antennas and frequency selective surfaces.

Analysis of terahertz chiral metamaterial was carried out by Fang *et al.* (2013). They designed a dual band THz chiral metamaterial using two different sizes of cross wires in the unit cell. The designed chiral metamaterial resonates at four different frequencies such as 4.8 THz, 5.6 THz, 7.9 THz and 8.2 THz. The designed structures were simulated using FEM based simulation software (CST MW Studio).

A novel hybrid H shaped metamaterial structure on a quartz substrate was proposed by Guo *et al.* (2013). The hybrid design of different sizes of H shaped structures in

each unit cell exhibits dual band property. The resonant frequencies of the proposed hybrid structure was (0.95 -1.01) THz and (1.26 – 1.42) THz. It was observed that there is a good agreement between the simulation results and THz-TDS measurement results.

3.3.3 Composite terahertz metamaterials

Singh *et al.* (2008) studied the effect of metal on transmission characteristics of THz metamaterials. Pb, Al, and Ag were considered as the test metals for analysis. The measurement and simulation result shows that Pb based metallic SRR with 300nm thickness provides 47.7% transmission where as Al, and Ag based SRR structure provides. 7%, 25.5%, and 14.1%, transmission respectively. THz time domain spectroscopy was used for measurements and CST Mw Studio was used for simulation.

Kubarev *et al.* (2009) conducted a study on the optical activity of metal-semiconductor microhelix structures arranged to form a two-dimensional array. Two structures were used for this study - one with microhelix structures on a GaAs medium and the other on silicon substrate. Maximum resonance was found at a wavelength that was twice the length of the microhelix - the fundamental resonant wavelength. Further, upon experimental investigation using direct interferometry, the refractive index at 2THz was found to be -0.11 due to chirality and resonance anomalous dispersion.

Lheurette *et al.* (2010) demonstrated negative refraction through a fishnet related metamaterial. Goniometric time domain spectroscopy system was used for measurements. An experimental characterization of a fishnet metamaterial design was proposed left handedness demonstration. Magnitude of the transmitted signal versus frequency for various angular positions of the detection antenna was reported. However the maximum transmitted signal corresponds to an angle of -1.6 degree and a frequency of 0.506 THz.

Liu *et al.* (2010) investigated and analyzed the interaction between a metamaterial and a THz electromagnetic wave. The design consisted of a unit cell made up of gold glued to the polyimide or GaAs substrate. 3D time domain finite-integration solver was used to simulate the structure having unit cells of different dimensions. Due to changes in transmission, abnormal characteristics appeared. Then a metamaterial structure composed of two distinct SRRs in a vertical direction was designed. The simulation results of their interaction with THz electromagnetic waves are analyzed. System resonated at frequencies between 0.5 THz and 2 THz. It was observed that only a single SRR is resonant at each of the two resonant frequencies.

Zhou *et al.* (2010) demonstrated optical activity in chiral metamaterials. A pair of jugated *Swastika* shaped metallic structures was used for design of chiral metama-

terial. Finite element method was used for simulation. Simulation results showed that there are two dips in the transmission spectra at 0.65 and 1 THz corresponding to a magnetic and an electric resonance. When the wave propagates through chiral metamaterial, there is a polarization rotation by 20 degree. Tunable chiral metamaterial design is useful in polarization controllers, circular polarizers for optoelectronic applications, life science microscopy and display applications.

Cia *et al.* (2011) designed 3-D metamaterials in the millimeter and terahertz (THz) frequency range. A fabrication technique to obtain low loss spatial 3D filters on polypropylene substrates using photolithography was proposed. Single and bi-layer SRR and CSRR screens were given to sustain the performance of polypropylene with resonant structures.

Zhang *et al.* (2012) realized a superconducting THz Metamaterial made from niobium nitride (NbN) films. They characterized the resonance properties of the metamaterial by using THz time-domain spectroscopy. Here they proposed two techniques to reduce the ohmic loss and to increase the quality factor Q of the resonance. Hence, they experimentally demonstrated unloaded quality factor (Q_u) of 178 at a temperature of 8K having resonance frequency 0.58 THz, which is 24 times as many as gold metamaterials with the same structure at the same temperature. The high Q_u performance of NbN MMs could remain fine at higher frequency of 1.02 THz. This application can solve the problem of loss in THz metamaterials and also lead to the development of THz devices based on superconducting film.

Zhang *et al.* (2009) developed an artificial dielectric structure, which consists of metal-mesh films layers embedded in polypropylene. Modification of the overall refractive index of the metamaterial by adjustment of geometry and spacing is shown. To demonstrate the usage they have designed a prototype broadband anti-reflection coating and applied to a single Z-cut quartz plate and did simulation by HFSS.

3.3.4 Tunable terahertz metamaterials

Waselikowski *et al.* (2011) showed a terahertz metamaterial, which is made up of three dimensional submillimeter-sized coils fabricated with an automated wire-bonder. Terahertz time domain spectroscopy method is used to find the response of the structure. Tunability of the metamaterial is showed by tuning of the Q-factor and resonance frequency by variation of the winding pitch of the coils.

Chowdhury *et al.* (2012) performed mode renormalization from odd order mode to even order mode through the design of reconfigurable split ring resonator. The design consists of a split ring resonator with silicon island placed in the gap. The conductivity in the gap could be varied through optical pumping. From the numeri-

cal simulations, it was observed that at higher pump powers the odd-modes dampen while the even-modes surfaces.

Kozlov *et al.* (2012) designed a metamaterial using a cubic dielectric resonator as the basic unit. A metallic strip with a gap was etched onto one side of this dielectric cube. Tuning is achieved by varying the electrical length of the metal strip, by photo-excitation of the gap or by voltage biasing. The structure was observed to act as a band pass filter with a pass-band from 0.45 THz to 0.5 THz.

Kowerdziej *et al.* (2012) developed and analyzed the performance of a metamaterial transducer that employs In-plane Switching Mode (IPS). The structure consists of a nematic liquid crystal sandwiched between two Ω shaped resonators. The orientation of the crystal can be controlled by providing an external bias voltage. This tuning enables one to make the refractive index positive, negative or zero. Furthermore, the band width over which the crystal displays negative refractive index can be tuned.

Ekmeki *et al.* (2011) examined frequency tunable metamaterials using broadside-coupled split ring resonators (BC-SRRs) at terahertz frequencies. For electrical excitation, the resonance frequency continuously redshifts as a function of displacement. A maximum frequency shift occurs for displacement of half a unit cell resulting in a shift of 663 GHz (51% of f_0).

Fan *et al.* (2011) proposed a tunable 3D metamaterial (DSRR) mounted on a sapphire substrate with silicon pad beneath gaps at terahertz frequencies. The optically tunable device act as a modulator or switch with 30% tuning of frequency and finds application in the far-infrared portion of the spectrum. In this paper, the fundamental resonant frequency was continuously tuned from 1.74 THz to 1.16 THz with increment of incident laser power.

Ozbey *et al.* (2011) designed a modified split ring resonator with a single end fixed cantilever incorporated into it. The cantilever can be dynamically controlled using an external magnetic field. This metamaterial presents the capability to be tuned over a continuous range of frequencies over wide bands rather than discreet frequencies or specific narrow bands. Two different designs were simulated and it was seen that one had a tuning frequency range from 0.147 to 0.275 THz and the other had a tuning range of 0.265 to 0.514 THz. The factors affecting the performance of the cantilever beam was also discussed.

Lee *et al.* (2013) designed a negative refractive index terahertz graphene metamaterial. The electrical modulation of the real part of refractive index of the designed metamaterial is -3.4 at 0.69 THz. It was shown that by electrical tuning of the graphene monolayer, the refractive index can be changed. Hence graphene as an active layer is a good choice for design of active terahertz metamaterials.

Odit *et al.* (2013) proposed the designs of two different metamaterial structures whose resonant frequency could be tuned using a MEMS cantilever. The first structure that was proposed was a U-shaped resonator consisting of three strips connected via cantilever beams, which has potential to be used as a tunable band-stop filter. When the bending angle of the cantilever beam was changed from 0° to 15° , the resonance frequency was found to change from 0.384THz to 0.586THz. In addition, a metamaterial that consists of a metal – dielectric – metal plate structure was also proposed. One metal plate was fabricated in such a way so as to behave as a cantilever beam. Hence, the distance between the two metal plates could be varied, which in turn varies the resonant frequency. The variation of the resonant frequency and transmission co-efficient with bending angle of the cantilever was simulated.

Bian *et al.* (2014) designed a tuneable metamaterial whose resonance is changed by changing the electric field. As in terahertz frequency the electronic and ionic polarizations are dominant, the dielectric constant of the substrate changes with frequency as well as the external electric field. The dielectric constant of the B-ST60 thin film substrate was decreased from 370 to 250 when the frequency increased from megahertz to terahertz. The simulation results of different dielectric constant and the corresponding transmission spectra were given, which provides a new possibility of designing active metamaterials.

3.4 Terahertz metamaterial switches

Tao *et al.* (2008a) proposed a terahertz metamaterial switch using a bimaterial cantilever placed at the capacitive gap of the SRR structure. The design and fabrication details of the switch design were also explained clearly. The measurement result shows that the resonance is strong at 0.75 THz. These types of dynamically controlled metamaterial structures have potential applications in the field of terahertz metamaterial devices such as tunable filters, phase shifters, switch etc.

Sheng *et al.* (2011b) proposed novel terahertz wave switch using metamaterial. Terahertz on–off switching is based on resonance characteristic of metamaterial, which is manipulated by modulated semiconductor laser. From the simulation, it was found that at 0.32 THz, the switch has on–off response time speed of 1 ms and extinction ratio of 19.4 dB.

Nanocomposite metamaterial are gaining momentum in the field of optical switches, sensors etc. Hajizadegan *et al.* (2012) designed a low loss, very fast, optical switch using a novel metamaterial structure. The nanocomposite nonlinear metamaterial structure provides a strong Kerr effect at a low pump power, which results 35 dB on/off ration of the switch.

Zhang *et al.* (2013b) studied the behavior of superconducting niobium nitride film at terahertz regime. NbN metamaterial of various thicknesses from 15 nm to 50nm were studied under terahertz pulse and an ultrafast modulation switching capability was observed. It was also observed that thicker NbN metamaterials show high quality factor and sharper resonance effects.

3.5 Terahertz metamaterial cloak

The exciting properties of metamaterial science are yielding a great interest among the scientific society in invisibility cloaking designs. Hiding an object from any other detecting device is the key to invisibility cloaking [Choudhury *et al.*, (2013a)]. This can be achieved when the incident EM wave bends around the object and comes out of the cloak without being scattered as shown in (Figure 8).

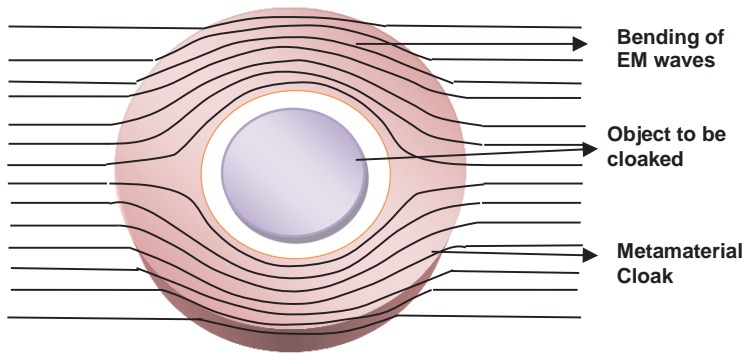


Figure 8: Schematic of an invisibility cloak.

The permeability and permittivity tensors of the cloak material are derived in such a way that the material becomes spatially invariant, anisotropic and inhomogeneous, the properties required to achieve cloaking. As the cloak is a multilayer structure, soft computing can be efficiently used for design of the cloak.

Tao *et al.* (2008c) proposed a terahertz metamaterial design for invisibility cloaking applications. A multilayer metamaterial based cylindrical invisibility cloak was designed using a commercially available multiphysics FEM solver. The structure was then fabricated. THz time domain spectroscopy was used for EM characterization of metamaterial unit cell and the measurement results are good agreement with the simulation results.

Jin *et al.* (2010) analyzed superconducting THz metamaterial having low loss. Normally at microwave, metamaterials made up of metallic structures have low losses and extraordinary properties. When the frequency is increased to THz, ohmic loss-

es also increase. At higher frequencies, superconducting metamaterial made up of Nb film was used to reduce losses. The simulation results showed that at 132 GHz and 418 GHz, the Q-factor of metamaterial, which is made up of superconducting Nb film is about 3 times as large as metamaterial, which is made up of Al film at 1K. These structures can use for fabrication of planar superlens and invisible cloaks in microwave as well as the THz functional devices.

Kildal *et al.* (2011) explained how gap waveguides can be used for an electromagnetic packaging technology with potential of reaching terahertz. The gap waveguides come from research on soft and hard surfaces for EBG surfaces and metamaterial cloaks.

Khodasevych *et al.* (2010) presented the design of a flexible fishnet metamaterial on a PDMS substrate operating at THz frequencies. PDMS has a low surface energy and is highly flexible. Full-wave finite element method was used for simulation. The transmittance was high at 2.1 THz. These flexible structures will be a suitable candidate for cloaking applications.

3.5 Metafoils

Meta-foils are flexible metamaterial designs having an array of metamaterial structures to achieve the desired properties. Moser *et al.* (2009) proposed a new design for metamaterial foil – one that is stronger, more flexible and can be used at wide angles of incidence. This new structure consists of S-shaped strings connected using metal thereby forming a structure in which metal plays the role of the conducting and structural material simultaneously. The various capacitances and inductances in the structure were discussed and a method to fabricate the same was presented. Using simulation, the resonant characteristics of the structure was studied and two resonant frequencies were observed- 3.2 THz (left handed resonance) and 6.8 THz (right-handed resonance). Further, a method to tune the meta-foil by adding dielectrics was discussed.

Moser *et al.* (2010) developed a meta-foil, a fully self-supported, locally stiff and globally flexible metamaterial. An array of parallel S-strings interconnected by transverse metal rods that are periodically repeated along the strings was the architecture used for meta-foil. UV or x-ray lithography based micro fabrication was used to manufacture the meta-foil. Fourier transform infrared spectroscopy was used to measure the spectra response. The simulation results showed resonance peaks at 3.6 and 5.4 THz. These meta-foils can be useful in sensors. It is suggested that if meta-foil material could be bent, it could be used as cylindrical hyperlens.

4 Conclusions

In this manuscript, terahertz design and fabrication issues have been explored along with their applications. An extensive literature survey has been carried out for metamaterial terahertz applications including metamaterial absorbers, filters, modulators, switches, lenses, and cloaking structures. The literature survey reveals that there is a natural breakpoint in terahertz domain where both the electric resonance, a characteristic of high frequency and the magnetic resonances, a characteristic of low frequency die out. This natural breakpoint brings about the use of artificial engineered materials called metamaterials for various applications.

It has been observed that most of the electromagnetic design procedure at terahertz regime follows a mechanism that involves scaling down of metamaterial structures designed for applications in microwave region. The scaling down technique was proved successful through experimental results.

Fabrication of the terahertz applications has been reported widely through standard techniques. However producing these devices on a large scale still remains to be a challenging task and should be explored. The study reveals that TDS is the most widely used technique for measurement and EM characterization of terahertz metamaterials. Although TDS measurement has been used successfully in most of the cases, these measurements are generally far-field measurements. This brings about a scope for developing near field measurement techniques.

References

- Alves, F.; Grbovic, D.; Kearney, B.; Lavrik, N. V.; Karunasiri, G.** (2013): Bi-material terahertz sensors using metamaterial structures. *Optics Express*, vol. 21, no. 11, pp. 13256-13271.
- Alves, F.; Kearney, B.; Grbovic, D.; Karunasiri, G.** (2012): Narrowband terahertz emitters using metamaterial films. *Optics Express*, vol. 20, no. 19, pp. 21025- 21032.
- Averitt, R. D.; Padilla, W. J.; Chen, H. T.; OHara, J. F.; Taylor, A. J.; Highstrete, C.; Lee, M.; Zide, J. M. O.; Bank, S. R.; Gossard, A. C.** (2007): Terahertz metamaterial devices. *Proceedings of SPIE*, vol. 6772, pp. 677209.
- Basiry, R.; Abiri, H.; Yahaghi, A.** (2012): Wide-band, stop-band and multi-band metamaterial filter design in terahertz frequencies. *Second Conference on Millimeter -Wave and Terahertz Technologies*, pp. 33-36.
- Capolino, F.** (2009): *Metamaterials Handbook: Theory and Phenomena of Metamaterials*. CRC Press, Taylor and Francis Group, New York, ISBN 978-9657001-9-4, 560p.

Chen, H. T.; Padilla, W. J.; Cich, M. J.; Azad, A. K.; Averitt, R. D.; Taylor, A. J. (2009): A metamaterial solid-state terahertz phase modulator. *Nature Photonics*, vol. 3, pp. 148-151.

Chen, M.; Zhang, Z.; Chan, K. T. (2009): Dual-band polarization-insensitive left-handed metamaterial in terahertz range. *Proceedings of 14th OptoElectronics and Communications Conference*, pp. 1-2.

Chen, W. C.; Mock, J. J.; Smith, D. R.; Akalin, T.; Padilla, W. J. (2011): Controlling Gigahertz and terahertz surface electromagnetic waves with metamaterial resonators. *Physical Review X*, vol. 1, pp. 021016(1)- 021016(6).

Chen, Y.; Naib, I. A. I. A.; Gu, J.; Wang, M.; Ozaki, T.; Morandotti, R.; Alves, W. Z.; Kearney, B.; Grbovic, D.; Karunasiri, G. (2012): Membrane metamaterial resonators with a sharp resonance: A comprehensive study towards practical terahertz filters and sensors. *AIP Advance*, pp. 022109(1)-022109(9).

Cheng, Y.; Huang, Q.; Nie, Y.; Gong, R. (2012): Terahertz chiral metamaterial based on complementary U-shaped structure. *Proceedings of 10th International Symposium on Antennas, Propagation & EM Theory*, pp. 706-709.

Chiam, S. Y.; Singh, R.; Rockstuh, C.; Lederer, F.; Zhang, W.; Bettiol, A. A. (2009): Analogue of electromagnetically induced transparency in a terahertz metamaterial. *Physical Review B*, vol. 80, pp. 153103(1)-153103(6).

Chicki, N.; Gennaro, E. D.; Esposito, E.; Andreone, A. (2009): Electron-beam lithographed metamaterial devices operating in the terahertz region. *Proceedings of IEEE International Workshop on Terahertz and mid Infrared Radiation: Basic Research and Practical Applications*, pp. 11-12.

Choudhury, B.; Jha, R. M. (2013a): A review on metamaterial invisibility cloaks. *Computers, Materials and Continua*, vol. 33, no. 3, pp. 287-308.

Choudhury, B.; Thiruvani B., Reddy, P. V.; Jha, R. M. (2013b): Soft computing techniques for Terahertz metamaterial RAM design for biomedical applications. *Computers, Materials and Continua*, vol. 37, no. 3, pp. 135-146.

Chowdhury, D. R.; Singh, R.; O'Hara, J. F.; Chen, H. T.; Taylor, A. J.; and Azad, A. K. (2012): Photo-doped silicon in split ring resonator gap towards dynamically reconfigurable terahertz metamaterial. *OCLEO Technical Digest*, 2p.

Chowdhury, D. R.; Singh, R.; Reiten, M. Zhou, J.; Taylor, A. J.; O'Hara, J. F. (2011): Tailored resonator coupling for modifying the terahertz metamaterial response. *Optics Express*, vol. 19, no. 11, pp. 10679-10685.

Cía, M. N.; Kuznetsov, S. A.; Aznabet, M.; Beruete, M.; Falcone, F.; Ayza, M. S. (2011): Route for bulk millimeter wave and terahertz metamaterial design. *IEEE Journal of Quantum Electronics*, vol. 47, no. 13, pp. 375-385.

- Cui, X.; Liu, H.; Wu, W.; Tang, Y.** (2010): A multi-band THz regime metamaterial design using a paired metallic circular-strip structure. *Proceedings of International Conference on Microwave and Millimeter Wave Technology (ICMMT)*, pp. 1781-1783.
- Ekmeki, E.; Strikwerda, A. C.; Fan, K.; Keiser, G.; Zhang, X.; Sayan, G. T.; Averitt, R. D.** (2011): Frequency tunable metamaterial designs using near field coupled srr structures in the terahertz region. *Proceedings of 36th International Conference on Infrared, Millimeter and Terahertz Waves (IRMMW-THz)*, pp. 1-2.
- Fan, K.; Strikwerda, A. C.; Tao, H.; Zhang, X.; Averitt, R. D.** (2011): A Tunable 3D Terahertz Metamaterial. *Proceedings of 36th International Conference on Infrared, Millimeter and Terahertz Waves (IRMMW-THz)*, pp. 1-2.
- Fang, F.; Cheng, Y.** (2013): Dual-band terahertz chiral metamaterial with giant optical activity and negative refractive index based on cross-wire structure. *Progress in Electromagnetic Research*, vol. 31, pp. 59-69.
- Ferguson, B.; Zhang, X. -C.** (2009): Materials for terahertz science and technology. *Nature Materials*, vol. 1, pp. 26-33.
- Gu, C.; Qu, S.; Pei, Z.; Zhou, H.; Wang, J.** (2010): A wide-band, polarization-insensitive and wide angle terahertz metamaterial absorber. *Progress In Electromagnetics Research Letters*, vol. 17, pp. 171-179.
- Guo, W.; He, L.; Sun, H.; Zhao, H.; Li, B.; Sun, X. W.** (2013): A dual-band terahertz metamaterial based on a hybrid 'H'-shaped cell. *Progress in Electromagnetic Research M*, vol. 30, pp. 39-50.
- Hajizadegan, M.; Sakhdari, M.; Ahmadi, V.** (2013): Design of a Kerr effect based terahertz all-optical switch using metallic nanocomposite metamaterial structure. *Proceedings of Second Conference on Millimeter-Wave and Terahertz Technologies*, pp. 5-8.
- Han, J.; Gu, J.; Lu, X.; Singh, R.; Tian, Z.; Xing, Q.; Zhang, W.** (2009): A close-ring pair terahertz metamaterial resonating at normal incidence. *Optics Express*, vol. 17, no. 22, pp. 20307- 20312.
- Hand, T. H.; Yuan, Y.; Palit, S.; Bingham, C.; Rahm, M.; Smith, D. R.; Padilla, W. J.; Jokerst, N.; Cummer, S. A.** (2008): Dual-band planar electric THz metamaterial with resonator yield analysis. *Proceedings of Conference on Lasers and Electro-Optics, and Conference on Quantum Electronics and Laser Science*, pp. 1-2.
- Hashimshony, D.; Zigler, A.; Papadopoulos, D.** (2001): Conversion of electrostatic to electromagnetic waves by superluminous ionization fronts. *Physical Review Letter*, vol. 86, pp. 2806 – 2809.

He, S.; Chen, T. (2013): Broadband THz Absorbers with graphene-based anisotropic metamaterial films. *IEEE Transactions on Terahertz Science and Technology*, vol. 3, pp. 1-7.

He, X. J.; Wang, Y.; Wang, J. M.; Gui, T. L. (2011): Dual-band terahertz metamaterial absorber with polarization insensitivity and wide incident. *Progress In Electromagnetics Research*, vol. 115, pp. 381-397.

Headland, D.; Withayachumnankul, W.; Webb, M.; Abbott, D. (2013): Beam deflection lens at terahertz frequencies using a hole lattice metamaterial. *Proceedings of 38th International Conference on Infrared, Millimeter, and Terahertz Waves*, pp. 1-2.

Hokmabadi, M. P.; Wilbert, D. S.; Kung, P.; Kim, S. M. (2013a): Analysis of terahertz metamaterial perfect absorber by using a novel quasi-static RLC circuit model. *38th International Conference on Infrared, Millimeter, and Terahertz Waves*, 2p.

Hokmabadi, M. P.; Wilbert, D. S.; Kung, P.; Kim, S. M. (2013b): Terahertz metamaterial absorbers. *Terahertz Science and Technology*, vol. 6, no. 1, pp. 40-58.

Horestani, A. K.; Withayachumnankul, W.; Chahadiah, A.; Ghaddar, A.; Zhar, M.; Abbott, D.; Akalin, T. (2013): Metamaterial-inspired bandpass filters for terahertz surface waves on Goubau Lines. *IEEE Transactions on Terahertz Science and Technology*, vol. 3, no. 6, pp. 851 – 858.

Hu, J. and Li, J. (2013): Equivalent circuit model research of terahertz wave absorber based on metamaterial. *Microwave Optical Technology Letters*, vol. 55, no.9, pp. 2195-2198.

Huang, W.; Lin, W.; Wang, L.; Chang, L.; Liao, C. (2012): Broadband optimization for a terahertz metamaterial absorber. *Proceedings of IEEE MTT-S International Microwave Workshop Series on Millimeter Wave Wireless Technology and Applications (IMWS)*, pp. 1- 3.

Jin, B.; Zhang, C.; Engelbrecht, S.; Pimenov, A.; Wu, J.; Xu, Q.; Cao, C.; Chen, J.; Xu, W.; Kang, L.; Wu, P. (2010): Low loss and magnetic field-tunable superconducting terahertz metamaterial. *Optics Express*, vol. 18, no. 16, pp. 17504 - 17509.

Kan, K.; Yang, J.; Ogata, A.; Kondoh, T.; Norizawa, K.; Yoshida, Y.; Hangyo, M.; Kuroda, R.; Toyokawa, H. (2012): Terahertz-wave generation using metamaterial and femtosecond electron bunch. *Proceedings of 37th International Conference on Infrared, Millimeter, and Terahertz Waves*, 2p.

Kearney, B.; Alves, F.; Grbovic, D.; Karunasiri, G. (2013): Terahertz metama-

terial absorbers with an embedded resistive layer. *Optical Materials Express*, vol. 3, no. 8, pp. 1020-1025.

Khodasevych, I. E.; Shah, C.M.; Rowe, W. S. T.; Mitchell, A. (2010): Flexible fishnet metamaterial on PDMS substrate for THz frequencies. *Proceedings of Conference on Optoelectronic and Microelectronic Materials and Devices*, pp. 25-26.

Kildal, P. S.; Maci, S.; Nogueira, A. V.; Kishk, A.; Iglesias, E. R. (2011): The gap waveguide as a metamaterial-based electromagnetic packaging technology enabling integration of MMICs and antennas up to terahertz. *EuCAP*, pp. 3715-3718.

Koutsoupidou, M.; Uzunoglu, N.; Karanasiou, I. S. (2012): Antennas on metamaterial substrates as emitting components for thz biomedical imaging. *Proceedings of the IEEE 12th International Conference on Bioinformatics & Bioengineering*, pp. 319-322.

Kowrdziejka, R.; Olifierczuka, M.; Salskib, B.; Parkaa, J. (2012): Tunable negative index metamaterial employing in-plane switching mode at terahertz frequencies. *Liquid Crystals*, vol. 39, no. 7, pp. 827-831.

Kozlov, D. S.; Odit, M. A.; Vendik, I. B.; Roh, Y. G.; Cheon, S.; Lee, C. W. (2013): Tunable terahertz metamaterial based on resonant dielectric inclusions with disturbed Mieresonance. *Applied Physics A: Materials Science and processing*, vol. 106, pp. 465- 470.

Kubarev, V. V.; Prinz, V. Y.; Naumova, E. V.; Golod, S .V. (2009): Terahertz optical activity and metamaterial properties of 2D array of metal-semiconductor microhelices. *Proceedings of 34th International Conference on Infrared, Millimeter, and Terahertz Waves*, 2p.

Kumara, N.; Strikwerdab, A.; Fanc, K.; Zhangc, X.; Averittb, R.; Plankena, P.; Adama, A. (2011): Direct measurement of the THz near-magnetic field of metamaterial elements. *Proceedings of 36th International Conference on Infrared, Millimeter and Terahertz Waves*, 2p.

Kung, P.; Kim, S. M. (2013): Terahertz metamaterial absorbers for sensing and imaging. *Proceedings of Progress in Electromagnetic Research*, pp. 232-235.

Lee, S. H.; Choi, J.; Kim, H.; Choi, H.; Min, B. (2013): Ultrafast refractive index control of a terahertz graphene metamaterial. *Scientific Reports*, pp. 1-6, DOI: 10.1038/srep02135.

Lheurette, E.; Garet, F.; Wang, S.; Blary, K.; Coutaz, J. L.; Lippens D. (2010): Wedge-type negative index metamaterial at 0.5 THz. *Proceedings of 35th International Conference on Infrared Millimeter and Terahertz Waves (IRMMW-THz)*, pp. 1-3.

Li, B.; He, L. X.; Yin, Y. Z.; Guo, W. Y.; Sun, X. W. (2012): A symmetrical dual-band terahertz meta-material with cruciform and square loops. *Progress In Electromagnetics Research C*, vol. 33, pp. 259-267.

Li, B.; He, L.; Yin, Y.; Guo, W.; Sun, X. (2013): An isotropy dual-band terahertz meta- material. *Microwave Optical Technology Letters*, vol. 55, no.5, pp. 988-990.

Lim, C. S.; Hong, M. H.; Chen, Z. C.; Han, N. R.; Luk'yanchuk, B.; Chong, T. C. (2010): Hybrid metamaterial design and fabrication for terahertz resonance response enhancement. *Optics Express*, vol. 8, no. 12, pp. 12421- 12429.

Liu, S. H.; Guo, L. X.; Li, J. C.; Ma, L. C. (2010): Dual-band SRR metamaterial in the terahertz regime. *Proceedings of 9th International Symposium on Antennas Propagation and EM Theory*, pp. 705-707.

Lu, M.; Li, W.; Brown, E. R. (2010): High-Order THz bandpass filters achieved by multilayer complementary metamaterial structures. *Proceedings of 35th International Conference on Infrared Millimeter and Terahertz Waves (IRMMW-THz)*, pp. 1-2.

Lu, Z.; Raga, B. C.; Islam, N. E. (2012): Design and analysis of a THz metamaterial structure with high refractive index at two frequencies. *Physics Research International*, vol. 2012, pp. 1- 9.

Maagt, P. (2007): Terahertz technology for space and earth applications. *Proceedings of International Workshop on Antenna Technology: Small and Smart Antenna, Metamaterials and Applications*, pp. 111-115.

Merbold, H.; Bitzer, A.; Enderli, F.; Feurer, T. (2011): Spatiotemporal visualization of THz near-fields in metamaterial arrays. *Infrared Milli Terahz Waves*, vol. 32, pp. 570-579.

Minowa, Y.; Fujii, T.; Nagai, M.; Ochiai, T.; Sakoda, K.; Hirao, K.; Tanaka, K. (2008): Evaluation of effective electric permittivity and magnetic permeability in metamaterial slabs by terahertz time-domain spectroscopy. *Optics Express*, vol. 16, no.7, pp. 4785 -4796.

Minowa, Y.; Nagai, M.; Tao, H.; Fan, K.; Strikwerda, A. C.; Zhang, X.; Averitt, R. D.; Tanaka, K. (2011): Extremely thin metamaterial as slab waveguide at terahertz frequencies. *IEEE Transactions on Terahertz Science And Technology*, vol. 1, no. 2, pp. 441-449.

Miyamaru, F.; Saito, Y.; Takeda, M. W.; Hou, B.; Liu, L.; Wen, W.; Sheng, P. (2008): Terahertz electric response of fractal metamaterial structures. *Physical Review B*, vol. 77, no. 4, pp. 045124(1) -045124(6).

Mo, M.; Wen, Q.; Chen, Z.; Yang, Q.; Jing, Y.; Zhang, H. (2013): Experimental demonstration of a broadband terahertz absorber using SiO₂ based metamaterial

structures. *Proceedings of IEEE Conference on Millimeter Waves and Terahertz Technology Workshop*, 2p.

Moser, O.; Casse, B. D. F.; Wilhelmi, O.; Saw, B. T. (2005): Terahertz response of a microfabricated rod-split-ring-resonator electromagnetic metamaterial. *Physical Review Letters*, vol. 94, pp. 063901(1)-063901(4).

Moser, H. O.; Jian, L. K.; Chen, H. S.; Bahou, M.; Kalaiselvi, S. M. P.; Virasawmy, S.; Maniam, S. M.; Cheng, X. X.; Heussler, S. P.; Mahmood, S. b.; Wu, B. I. (2009): All-metal self-supported THz metamaterial the meta foil. *Optics Express*, vol. 17, no. 26, pp. 23914- 23919.

Moser, H. O.; Jian, L. K.; Chen, H. S.; Bahou, M.; Kalaiselvi, S. M. P.; Virasawmy, S.; Cheng, X. X.; Banas, A.; Banas, K.; Heussler, S. P.; Wu, B. I.; Zhang, W .B.; Maniam, S. M.; Hua, W. (2010): THz meta foil a platform for practical applications of metamaterials. *Journal of Modern Optics*, vol. 57, no. 19, pp. 1936–1943.

Neu, J.; Krolla, B.; Paul, O.; Reinhard, B.; Beigang, R.; Rahm, M. (2010): Metamaterial based gradient index lens with strong focusing in the THz frequency range. *Optics Express*, vol. 18, issue 26, pp. 27748-27757.

Noor, A.; Hu, Z. (2010): Study of wideband, wide angle, polarization independent metamaterial Hilbert curve absorbing screen for terahertz bolometers. *Infrared Milli Terahertz Waves*, vol. 31, pp. 791–798.

Odit, M. A.; Vendik, I. B.; Kozlov, D. S.; Munina, I. V.; Turgaliev, V. M. (2012): Tunable metamaterial structures for controlling THz radiation. *Proceedings of IEEE Conference MSMW '13*, pp. 40 - 44.

Olifierczuk, M.; Kowrdziej, R.; Jaroszewicz, L.; Czerwinski, M.; Parka, J. (2012): Numerical analysis of THz metamaterial with high birefringence liquid crystal. *Liquid Crystals*, vol. 39, no. 6, pp. 739- 744.

Ortner, A.; Bitzer, A.; Walther, M. (2010): THz near-field microscopy of complementary metamaterial structures: Babinet's Principle. *Proceedings of European Optical Society Annual Meeting*, 2p.

Ozbey, B.; Aktas, O. (2011): Continuously tunable terahertz metamaterial employing magnetically actuated cantilevers. *Optics Express*, vol. 19, no. 7, pp. 5741-5742.

Padilla, W. J.; Taylor, A. J., Highstrete, C.; Lee; M.; Averitt, R. D. (2006): Dynamical electric and magnetic metamaterial response at terahertz frequencies. *Physical Review Letters*, vol. 96, no. 10, pp. 107401(1)-107401(4).

Padilla, W. J. (2009): Metamaterial devices for the terahertz gap. *Proceedings of Asia Pacific Microwave Conference, APMC 2009*, pp. 1297-1298.

Park, K. Y.; Wiwatcharagoses, N.; Baczewski, A.; Chahal, P. (2011): A novel terahertz power meter using metamaterial-inspired thin-film absorber. *Proceedings of 36th International Conference on Infrared, Millimeter and Terahertz Waves (IRMMW-THz)*, pp. 1-2.

Paul, O.; Imhof, C.; Reinhard, B.; Zengerle, R.; Beigang, R. (2008): Bulk negative index metamaterial operating at THz frequencies. *Proceedings of 33rd International Conference on Infrared, Millimeter and Terahertz Waves, IRMMW-THz*, pp. 1-2.

Paul, O.; Imhof, C.; Lägel, B.; Wolff, S.; Heinrich, J.; Höfling, S.; Forchel, A.; Zengerle, R.; Beigang, R.; Rahm, M. (2009): Electrically tunable metamaterial for polarization-independent terahertz modulation. *Proceedings of Conference on Lasers and Electro-Optics, and Conference on Quantum electronics and Laser Science Conferenc*, pp. 1-2.

Reinhard, B.; Schmitt, K. M.; Wollrab, V.; Neu1, J.; Beigang, R.; Rahm, M. (2012): Terahertz thin film and refractive index sensing with a metamaterial near-field sensor. *Proceedings of 37th International Conference on Infrared, Millimeter, and Terahertz Waves (IRMMW-THz)*, pp. 1- 2.

Rout, S.; Shrekenhamer, D.; Sonkusale, S.; Padilla, W. (2010): Embedded HEMT/metamaterial composite devices for active terahertz modulation. *Proceedings of 23rd Annual Meeting of the IEEE Photonics Society*, pp. 437-438.

Sabah, C.; Roskos, H. G. (2009): Broadband terahertz metamaterial for negative refraction. *Progress In Electromagnetics Research Symposium Proceedings*, pp. 785-788.

Sabah, C.; Roskos, H. G. (2011a): Periodic array of chiral metamaterial-dielectric slabs for the application as terahertz polarization rotator. *Proceedings of XXXth URSI General Assembly and Scientific Symposium*, pp 1-4.

Sabah, C.; Roskos, H. G. (2011b): Dual-band polarization-independent fishnet metamaterial for terahertz frequency range. *Proceedings of 36th International Conference on Infrared, Millimeter and Terahertz Waves (IRMMW-THz)*, pp. 1-2.

Sabah, C.; Roskos, H. G. (2011c): Terahertz polarization rotator consists of chiral metamaterial and dielectric slabs. *Proceedings of 36th International Conference on Infrared, Millimeter and Terahertz Waves (IRMMW-THz)*, pp 1-2.

Shchegolkov, D. Y.; Azad, A. K.; O'Hara, J. F.; Simakov, E. I. (2010): Perfect subwavelength fishnet like metamaterial-based film terahertz absorbers. *Physical Review B*, vol. 82, pp. 205117(1)-205117(6).

Sheng, L. J.; Jun, L. J. (2011a): A novel terahertz wave switch based on metamaterial. *Microwave And Optical Technology Letters*, vol. 53, no. 3, pp. 276-278.

- Sheng, L. J.; Li, Z. X.** (2011*b*): Terahertz wave modulator based on metamaterial. *Journal of Physics: Conference Series*, vol. 276, pp. 012213 (1)-012213 (3).
- Shin, Y.** (2011): Composite metamaterial waveguides for THz sheet beam devices. *Proceedings of 36th International Conference on Infrared, Millimeter and Terahertz Waves (IRMMW-THz)*, pp. 1-2.
- Shin, Y. M.; Baig, A.; Spear, A.; Zhao, J.; Gamzina, D.; Domier, C. W.; Luhmann Jr, N. C.** (2010): MEMS fabrications of broadband epsilon negative (ENG) metamaterial electronic circuit for 0.22 THz sheet beam TWT application. *Proceedings of 35th International Conference on Infrared Millimeter and Terahertz Waves (IRMMW-THz)*, pp. 1-2.
- Siegel, P. H.** (2004): Terahertz technology in biology and medicine. *IEEE Transactions on Microwave Theory and Techniques*, vol. 52, no. 2, pp., 2438-2447.
- Singh, N.; Tuniz, A.; Lwin, R.; Atakaramians, S.; Argyros, A.; Fleming, S. C.; Kuhlmeiy, B. T.** (2012): Drawn double split ring magnetic metamaterial in terahertz range. *Proceedings of 37th International Conference on Infrared, Millimeter, and Terahertz Waves (IRMMW-THz)*, 2p.
- Singh, R.; Azad, A. K.; Zhang, W.** (2008): Influence of metal permittivity on transmission properties of terahertz metamaterials. *Proceedings of Conference on Lasers and Electro-Optics, and Conference on Quantum Electronics and Laser Science*, pp. 1-2.
- Singh, R.; Tian, Z.; Han, J.; Rockstuhl, C.; Gu, J.; Zhang, W.** (2010): Planar terahertz metamaterial at cryogenic temperatures. *Proceedings of Conference on Lasers and Electro-Optics (CLEO) and Quantum Electronics and Laser Science Conference (QELS)*, pp. 1-2.
- Smith, D. R.; Pendry, J. B.; Wiltshire, M. C. K.** (2004): Metamaterials and negative refractive index. *Science*, vol. 305, pp. 788-792.
- Starinshak, D. P.; Wilson, J. D.; Chevalier, C. T.** (2007): Investigating holey metamaterial effects in terahertz traveling-wave tube amplifier, NASA/TP 2007-214701, pp. 1-9.
- Strikwerda, A. C.; Tao, H.; Kadlec, E. A.; Fan, K.; Padilla, W. J.; Averitt, R. D.; Shaner, E. A.; Zhang, X.** (2011): Metamaterial based terahertz detector. *Proceedings of 36th International Conference on Infrared, Millimeter and Terahertz Waves (IRMMW-THz)*, pp. 1-2.
- Tao, H.; Strikwerda, A.; Bingham, C.; Padilla, W. J.; Zhang, X.; Averitt, R. D.** (2008*a*): Dynamical control of terahertz metamaterial resonance response using bimaterial cantilevers. *Proceedings of Progress In Electromagnetics Research Symposium*, pp. 870-873.

Tao, H.; Bingham, C. M.; Strikwerda, A. C.; Pilon, D.; Shrekenhamer, D.; Landy, N. I.; Fan, K.; Zhang, X.; Padilla, W. J.; Averitt, R. D. (2008b): Highly flexible wide angle of incidence terahertz metamaterial absorber: Design, fabrication, and characterization. *Physical Review B*, pp. 241103(1) – 241103(4).

Tao, H.; Landy, N. I.; Fan, K.; Strikwerda, A. C.; Padilla, W. J.; Averitt, R. D.; Zhang, X. (2008c): Flexible terahertz metamaterials: Towards a terahertz metamaterial invisible cloak. *Proceedings of IEEE International Electron Devices Meeting*, pp. 1-4.

Tao, H.; Amsden, J. J.; Strikwerda, A. C.; Fan, K.; Kaplan, D. L.; Zhang, X.; Averitt, R. D.; Omenetto, F. G. (2010): Metamaterial silk composites at terahertz frequencies. *Advanced Materials*, vol. 22, pp. 3527–3531.

Tavallae, A. A.; Hon, P.W. C.; Mehta, K.; Itoh, T.; Williams, B. S. (2010): Zero-Index Terahertz quantum-cascade metamaterial lasers. *IEEE Journal of Quantum Electronics*, vol. 46, no. 7, pp. 1091-1098.

Wallauer, J.; Bitzer, A.; Waselikowski, S.; Walther, M. (2011): Near-field signature of electromagnetic coupling in metamaterial arrays: A terahertz microscopy study. *Optics Express*, vol. 276, vol. 19, no. 18, pp. 17283 - 17292.

Wang, J.; Wang, S.; Singh, R.; Zhang, W. (2013): Metamaterial inspired terahertz devices: from ultra-sensitive sensing to near field manipulation. *Chinese Optics Letters*, vol. 11, pp. 1183 - 1189.

Waselikowski, S.; Kratt, K.; Badilita, V.; Wallrabe, U.; Korvink, J. G.; Walther, M. (2011): Terahertz metamaterial consisting of three-dimensional microcoils. *Proceedings of Metamaterials: The Fifth International Congress on Advanced Electromagnetic Materials in Microwaves and Optics*, pp. 122-124.

Xie, Y.; Li, Y.; Liu, Y.; Zhang, H.; Wen, Q. (2009): The design of a terahertz metamaterial absorber basing on LTCC technology. *Proceedings of International Conference on Electronic Packaging Technology & High Density Packaging (ICEPT-HDP)*, pp. 494-496.

Yang, T.; Li, X.; Zhu, W. (2013): A tunable metamaterial absorber employing mems actuators in THz regime. *Proceedings of 8th IEEE International Conference on Nano/Micro Engineered and Molecular Systems (NEMS)*, pp. 829-832.

Yuan, Y.; Bingham, C.; Talmage, T.; Palit, S. (2008): A dual-resonant terahertz metamaterial based on single-particle electric-field-coupled resonators. *Applied Physics Letter*, vol. 93, no. 19, pp. 191110(1)- 191110(3).

Zhang, C. H.; Wu, J. B.; Jin, B. B.; Ji, Z. M.; Kang, L.; Xu, W. W.; Chen, J.; Tonouchi, M.; Wu, P. H. (2012): Low-loss terahertz metamaterial from superconducting niobium nitride films. *Optics Express*, vol. 20, issue 1, pp. 42-47.

Zhang, J.; Ade, P. A. R.; Mauskopf, P.; Monceli, L.; Savini, G.; Whitehouse, N. (2009): New artificial dielectric metamaterial and its application as a THz antireflection coating. *Applied Optics*, vol. 48, issue 35, pp. 6635-6642.

Zhang, W.; Zhu, W. M.; Cai, H.; Kropelnicki, P.; Randles, A. B.; Tang, M.; Tanoto, H.; Wu, Q. Y.; Teng, J. H.; Zhang, X. H.; Kwong, D. L.; Liu, A. Q. (2013a): A tunable MEMS THz waveplate based on isotropicity dependent metamaterial. *Proceedings of IEEE Conference on Transducers*, pp. 538 - 541.

Zhang, C.; Jin, B.; Han, J.; Kawayama, I.; Murakami, H.; Jia, X.; Liang, L.; Kang, L.; Chen, J.; Tonouchi, M.; Wu, P.(2013b): Nonlinear response of superconducting NbN thin film and NbN metamaterial induced by intense terahertz pulses. *New Journal of Physics*, vol. 15, pp. 155017 - 155028.

Zhou, J.; Chowdhury, R.; Zhao, R.; Soukoulis, C. M.; Taylor, A. J.; Hara, J. O'. (2010): Chiral THz metamaterial with tunable optical activity. *Proceedings of Conference on Lasers and Electro-Optics paper CTuF*, 2p.

